Intracellular Ca^{2+} stores in chick cerebellum Purkinje neurons: ontogenetic and functional studies

ROBERTA SACCHETTO, KENNETH D. CLIFFER, PAOLA PODINI, ANTONELLO VILLA, BURGESS N. CHRISTENSEN, AND POMPEO VOLPE

Centro di Studio per la Biologia e la Fisiopatologia Muscolare del Consiglio Nazionale delle Ricerca, Dipartimento di Scienze Biomediche Sperimentali dell'Università di Padova, 35121 Padua; Dipartimento di Farmacologia dell'Università di Milano, Dibit Istituto Scientifico San Raffaele, 20132 Milan; Istituto Pluridisciplinare di Patologia Generale dell'Università di Messina, 98100 Messina, Italy; and Department of Physiology and Biophysics, University of Texas Medical Branch, Galveston, Texas 77555

Sacchetto, Roberta, Kenneth D. Cliffer, Paola Podini, Antonello Villa, Burgess N. Christensen, and Pompeo Volpe. Intracellular Ca^{2+} stores in chick cerebellum Purkinje neurons: ontogenetic and functional studies. *Am. J. Physiol.* 269 (*Cell Physiol.* 38): C1219–C1227, 1995.—The molecular composition of intracellular Ca^{2+} stores in developing chicken cerebellum Purkinje neurons from *embryonic day 11* (*E11*) to *posthatching day 2* (*P2*) was studied by immunocytochemistry using specific antibodies for three molecular constituents, the receptor (R) and/or channel sensitive to inositol 1,4,5-trisphosphate (IP_3), Ca^{2+}-adenosinetriphosphatase (ATPase), and calsequestrin (CS). CS, IP_3R, and Ca^{2+}-ATPase were first detected by light-microscopic immunofluorescence in migrating Purkinje cells at *E11–E12* and throughout late phases of embryonic development. Ontogenesis of CS, IP_3R, and Ca^{2+}-ATPase accompanied well-defined stages of cerebellum histogenesis and cytogenesis and was accomplished before hatching. High-resolution immunogold electronmicroscopy revealed that, at *E18–P1*, CS was still largely distributed to the endoplasmic reticulum (ER) lumen and began to be segregated to ER subcompartments (calciosomes) only by *P2*, whereas the IP_3R was concentrated into ER cisternal stacks as early as *E18*. Both ionotropic and metabotropic plasma membrane receptors were present in dissociated single chicken Purkinje cells from *E16* onward, as indicated by measurements of membrane currents (whole cell recording mode) and of cytoplasmic Ca^{2+} transients monitored with the cell-trappable fluorescent indicator fura 2-acetoxymethyl ester, respectively. Cytoplasmic Ca^{2+} transients were detected after either activation of glutamate metabotropic receptors, i.e., evidence of IP_3-sensitive Ca^{2+} channels, or application of caffeine, i.e., evidence of ryanodine-sensitive Ca^{2+} channels. Intracellular Ca^{2+} stores appear to be functional during embryonic development.

calcium channels; calcium homeostasis; development

ONE OF THE KEY PHENOMENA in cell physiology is the control of intracellular Ca^{2+} homeostasis (20). Redistribution of Ca^{2+} from intracellular rapidly exchanging Ca^{2+} stores plays a pivotal role in several cellular functions. Cerebellum Purkinje neurons of the chicken are a good experimental model for the ultrastructural, molecular, and functional study of rapidly exchanging Ca^{2+} stores (20), since they are richly endowed with the molecular components involved in uptake, release and storage of Ca^{2+}, i.e., Ca^{2+} pumps, Ca^{2+} release channels, and intraluminal low-affinity, high-capacity Ca^{2+} binding proteins (4, 5, 9, 14, 28, 30–36). Such Ca^{2+} stores represent specialized subcompartments of the endoplasmic reticulum (ER) (20, 28, 30, 37). Until now, they have been investigated in adult chicken or in chicks. The prenatal development and function of Ca^{2+} stores, however, have never been studied.

Purkinje neurons and neurons of the deep nuclei derive from a primary cell matrix in the neural epithelium covering the surface of the fourth ventricle (for reviews see Refs. 2, 7, 16). Postmitotic precursors of Purkinje neurons acquire bipolar shape and attain their final destination after an outwardly radial migration (cf. Refs. 1, 7). Upon reaching the primordial Purkinje cell layer [between *embryonic days 12* and *14* (*E12* and *E14*, respectively)], simple-fusiform neurons begin to differentiate into complex-fusiform neurons and then into stellate cells with randomly organized dendrites. Before hatching, the soma of Purkinje cells are arranged in a single regular monolayer and dendritic trees attain adequate development and proper orientation perpendicular to the major axis of the folia (1, 2, 16, 21, 22).

Cytogenesis and histogenesis of the cerebellum, in particular dendritic growth and synaptogenesis of Purkinje cells, proceed in parallel with the assembly of neuronal circuits. It is also well established that cerebellar cytogenesis is not ruled by phyletic factors but by the functional requirement of the species, and the length of histogenesis is influenced by the character of the offspring (2). Thus, in the nidifugous chick (apt offspring), functionality and morphological maturation are attained before hatching.

Differentiation of Purkinje cells requires a massive reprogramming of gene expression. In the present study, we have monitored in chicken cerebellum, from *E11* to *postnatal day 2* (*P2*), the ontogenetic expression of calsequestrin (CS), inositol 1,4,5-trisphosphate receptor (IP_3R), and Ca^{2+}-adenosinetriphosphatase (ATPase), three constituents of rapidly exchanging, intracellular Ca^{2+} stores (28, 30, 32, 35). CS, IP_3R and Ca^{2+}-ATPase are first detected in migrating Purkinje cells at *E11–E12* and throughout late phases of embryonic development. Ontogenesis of CS, IP_3R, and Ca^{2+}-ATPase was found to accompany well-defined stages of cerebellum histogenesis and cytogenesis. In the present study, we also provide a first insight into the biogenesis of membrane subcompartments specialized for intracellular Ca^{2+} homeostasis by means of high-resolution immunogold electron microscopy: CS at *E18–P1* was largely distributed to the ER lumen and began to be segregated

to ER subcompartments (calciosomes) by *P2*, whereas IP_3R appeared to be distributed to ER cisternae and stacks as early as *E18*. Finally, measurements of membrane currents and of cytoplasmic Ca^{2+} transients in acutely dissociated, single chicken Purkinje cells from *E16* onward indicated that both ionotropic and metabotropic excitatory amino acid receptors are functional and that intracellular Ca^{2+} stores are fully operative.

Evidence is thus provided that morphological and functional maturation of intracellular Ca^{2+} stores is attained concomitantly during prenatal development of chicken Purkinje neurons.

MATERIALS AND METHODS

Immunofluorescence. The cerebellum was quickly removed from 2-mo-old adult chickens, embryonic chicks (*E11* onward), and posthatching chicks (*P1* and *P2*). Cerebellar cortex was immediately fixed with a mixture of 4% paraformaldeyde-0.25% glutaraldeyde and processed as previously described (18, 30). Cerebellum cortex parasagittal 10-μm-thick sections were stained by immunofluorescence with rabbit anti-(chicken skeletal muscle CS) polyclonal antibodies (35), rabbit anti-IP_3R polyclonal antibodies (18) and mouse anti-Ca^{2+} ATPase monoclonal antibodies (30, 31) using anti-rabbit immunoglobulin (Ig) G or anti-mouse IgG conjugated to rhodamine. Anti-IP_3R antibodies were elicited against the synthetic 19-amino acid peptide of the COOH-terminal and recognize the predominant type I IP_3R isoform (13). Antibody specificity has been previously shown in Volpe et al. (31, 32, 35) and Nori et al. (18).

Immunogold electron microscopy. Experiments were performed exactly as described in Villa et al. (30). Briefly, ultrathin cryosections (50–100 nm) were exposed to either anti-CS or anti-IP_3R antibodies for 1 h at 37°C, washed with phosphate-glycine buffer, and decorated with anti-IgG-coated 5-nm gold particles (30). Cryosections were examined in a Hitachi H-7000 electron microscope.

Purkinje cell preparation. Cells were prepared from chick embryos (*E16* to hatching). The highest yields of viable identifiable Purkinje cells were obtained from embryos from *E17* to hatching. Earlier embryos had fewer Purkinje cells differentiated enough to be clearly identifiable.

An embryo was removed from the egg, the skin over the caudal part of the skull was incised, the skull was opened, and the cerebellum was scooped out with a cold spatula and placed immediately into continuously oxygenated cold modified chick Tyrode solution [MCTS; containing 154 mM NaCl, 2.68 mM KCl, 6 mM $MgCl_2$, 1.8 mM $CaCl_2$, 15 mM dextrose, and 10 mM *N*-2-hydroxyethylpiperazine-*N'*-2-ethanesulfonic acid (HEPES), pH 7.4].

Parasagittal slices ~1 mm thick were obtained with a razor blade and, after removal of the tips of the folia, placed into oxygenated MCTS at room temperature for variable periods (5 min to 2 h). Tissue pieces were treated for 0.5–1 h with papain in Earle's balanced salt solution (EBSS; 20 U/ml in 1 mM L-cysteine with 0.5 mM EDTA) at 37°C, equilibrated for pH 7–8 with 95% O_2-5% CO_2, and then transferred to an albumin-ovomucoid inhibitor solution in EBSS, in which they were held at room temperature under the O_2-CO_2 mixture until used (up to 30 h).

Papain-treated tissue was gently triturated in MCTS through a series of fire-polished glass pipettes of decreasing bore size to dissociate the cells mechanically. Dissociated cells were then placed in the appropriate chamber for either electrophysiological recordings or cytoplasmic Ca^{2+} measurements. Purkinje cells were identified by the large size of their somata (12–30 μm diam) and their characteristic shape, with a rounded cell body and a single primary dendrite. Usually secondary and higher order (and sometimes primary) dendrites were not evident. Often the axon was visible opposite the primary dendrite.

Electrophysiological recording. High-resistance seals on cell somata were made with patch pipettes using gentle suction; electrode resistance measured 2–4 MΩ. Patch pipettes contained 70 mM CsCl, 70 mM CsFl, 0.2 mM $CaCl_2$, 11 mM ethylene glycol-bis(β-aminoethyl ether)-*N,N,N',N'*-tetraacetic acid, and 10 mM HEPES (pH 7.4 with CsOH) and coaxed into whole cell recording mode (8) using current pulses and/or additional suction. Cells were clamped at −70 mV and moved into a separate tubular compartment of the recording chamber (internal volume ~200 μl) in which the surrounding fluid could be rapidly changed (20–40 ms). This change was achieved using a gravity-driven siphon fitted with a solenoid-activated microvalve to start and stop the flow and with a needle valve to regulate flow rate. A flow rate between 1.5 and 4.0 ml/min was used to establish an effective concentration clamp with regard to the composition of the applied fluid bathing the cell.

Data were recorded on a videocassette recorder via a digital audio processor for later replay and analysis.

Cytoplasmic Ca^{2+} measurements by microfluorimetry. Dissociated cells were plated in a recording chamber with a no. 1 coverslip serving as the bottom. Cells were incubated in fura 2-acetoxymethyl ester (AM; 2–4 μM) for at least 30 min. A chosen cell soma was centered in the field of an oil-immersion objective (×63, NA 1.2) of a Nikon inverted microscope equipped for epifluorescence. A split-beam fiber optic system leading from a xenon lamp was designed to alternately expose the cell to 340- and 380-nm excitation, 1 s each (for a 2-s cycle), through electronically operated shutters. Emitted photons were measured by a photomultiplier tube connected to one of the photography ports on the microscope. Measurements were fed to a computer for storage on disk and subsequent analysis.

The system was calibrated for the relationship between fura 2 emission during excitation at 340 and 380 nm and the Ca^{2+} concentration using Ca^{2+} buffers in a dish (Molecular Probes). In this study, calibration of individual cells using ionophores was not carried out. Although the accepted relationship involves a formula incorporating the maximum and the minimum emission ratio (6), the relationship of Ca^{2+} concentration to the emission ratio was essentially linear in the range 0–350 nM Ca^{2+} (0.22–1.93 ratio, $r^2 = 0.9991$). The fitted line had a formula of $[Ca^{2+}] = 203 \cdot R - 45$, where $[Ca^{2+}]$ is the Ca^{2+} nanomolar concentration and R is the ratio of emission during excitation at 340 nm divided by that during excitation at 380 nm. Given the highly questionable relationship between the enviroment of Ca^{2+} during calibration and that in a living cell, only the ratio is reported in Figs. 6 and 7, as a measure of relative Ca^{2+} concentration.

Solutions, containing either *trans*-(1*S*,3*R*)-1-aminocyclopentane-1,3-dicarboxylic acid (ACPD) or caffeine, were applied using a picospritzer (General Valve) through a micropipette located near the cell.

RESULTS

Ontogenetic expression of CS in chicken cerebellum. As has been known since the pioneer studies of Ramon y Cajal (22), Purkinje cells do not mature synchronously. The morphological description of such cells on the basis of pure chronological criteria may thus be misleading (1). The predominant morphological features, as evidenced by immunofluorescence, will be described with respect to defined embryonic ages.

At *E12*, CS-immunolabeled cells appear mostly round shaped and distributed in multiple layers underneath the cerebellar cortex molecular layer (Fig. 1*A*). Nuclei are often recognizable as unstained areas, whereas cytoplasmatic processes are evident in a few cases (arrow in Fig. 1*B* indicates a process emerging from the apical pole) because of the plane section.

At *E14*, Purkinje cells are aligned in an almost regular single layer (Fig. 1, *C* and *D*) and can be seen as round-shaped cells (Fig. 1*D*) or typical bipolar cells (Fig. 1*C*). At higher magnification, bipolar cells are readily identified, i.e., oval soma with smooth contours from which emerge two opposite cytoplasmic processes. Apical and basal processes are best seen (Fig. 1*E*) as well as bifurcations of apical ones (Fig. 1*F*).

At *E18*, Purkinje neurons are aligned into a monolayer, and their dendritic trees penetrate into the molecular layer with proper orientation (Fig. 1*G*). Dendritic

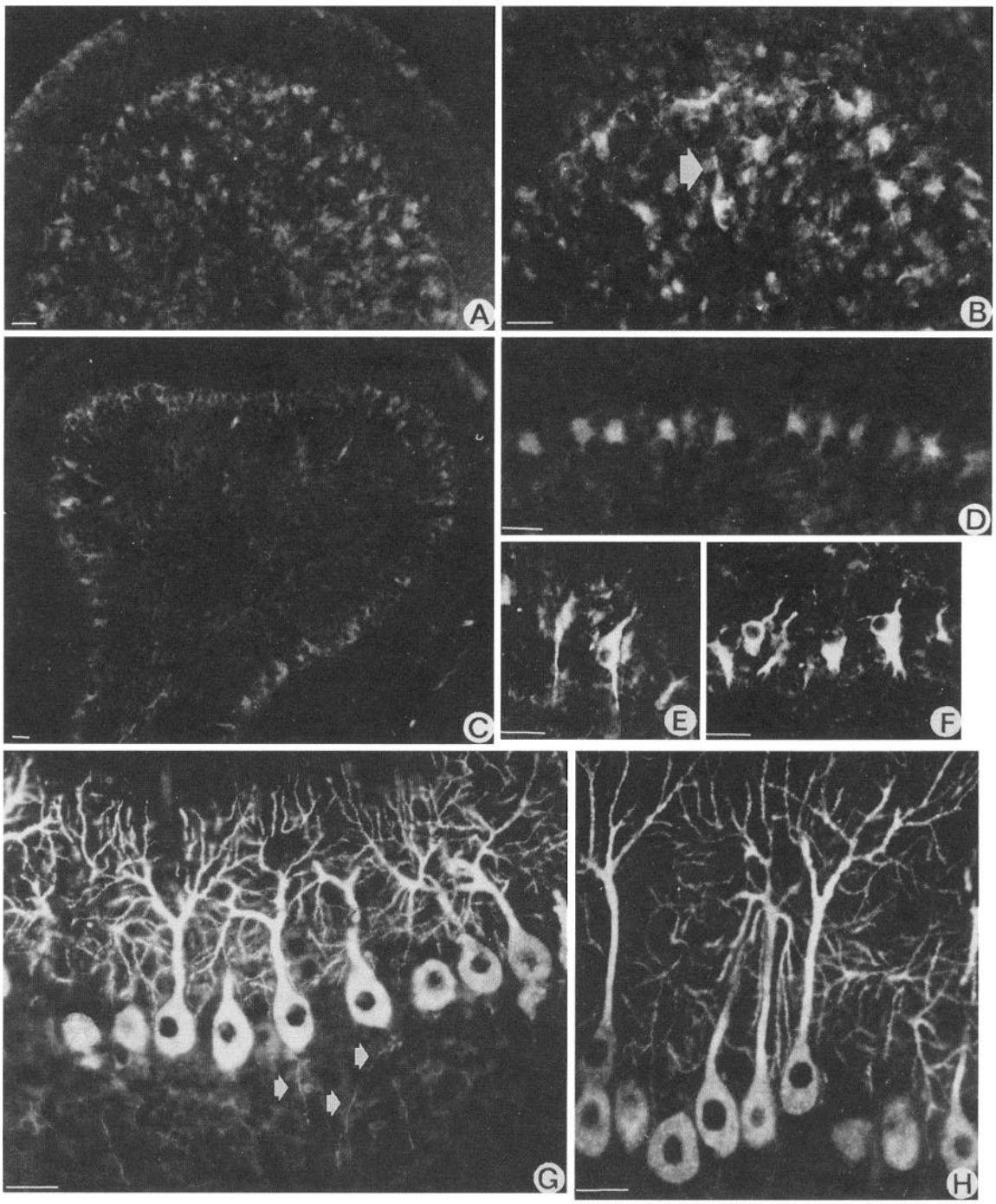

Fig. 1. Calsequestrin immunofluorescence of Purkinje neurons in developing chicken cerebellum. *A* and *B*: *embryonic day 12* (*E12*); *C–F*: *E14*; *C* and *D*: Purkinje cell layer outlined by Purkinje cell soma; *E* and *F*: details of Purkinje cells. *G*: *E18*; *H*: *posthatching day 1* (*P1*). Marked labeling of both soma and dentritic trees is evident. Axons traveling through molecular layer of cerebellum cortex are indicated by arrows in *G*. Bar = 20 μm.

arborization does not yet extend the full depth of the molecular layer (Fig. 1*G*). At *P1*, full-length dendritic trees are attained (Fig. 1*H*).

Ontogenetic expression of IP_3R in chicken cerebellum. Immunofluorescence of cerebellar cortex with anti-IP_3R antibodies is shown in Fig. 2. At *E11* and *E12*, clusters of IP_3R-positive round-shaped cells are observed (Fig. 2, *B* and *A*) in the process of outward migration. At *E14*, Purkinje neurons are disposed at the interface between the molecular and granule layer and have assumed a more defined pearlike morphology (Fig. 2*C*). Apical processes are still bulky and show a few branches (arrows in Fig. 2, *D* and *E*). At *E15*, the dendritic tree begins to unfold from the vertical main apical shaft with primary branches and short secondary branches (Fig. 2*F*) and is well developed by *E18* (Fig. 2*G*). No apparent difference is observed between *P1* (Fig. 2*H*) and adult cerebellum Purkinje neurons (not shown) with respect to alignment of soma, size, and branching of dendritic trees (28).

Ontogenetic expression of Ca^{2+}-ATPase in chicken cerebellum. At *E11*, Ca^{2+}-ATPase is expressed in Purkinje neurons (Fig. 3*A*) and in neurons of the deep nuclei (Fig. 3*B*). The latter neurons are completely differentiated by *E18* (2), as also shown in Fig. 3*D*. At *E18*, Purkinje neurons are aligned into a monolayer, and their dendritic trees penetrate into the molecular layer with proper orientation (Fig. 3*C*). Morphology of Purkinje neurons at *E18* and *P1* (not shown) was virtually identical.

CS and IP_3R immunogold labeling. Immunogold decoration of ultrathin cryosections (Fig. 4) was employed to investigate Purkinje neurons between *E18* and *P2* (somata in Fig. 4, *A–C*, *F*, and *G*; dendrites in Fig. 4,

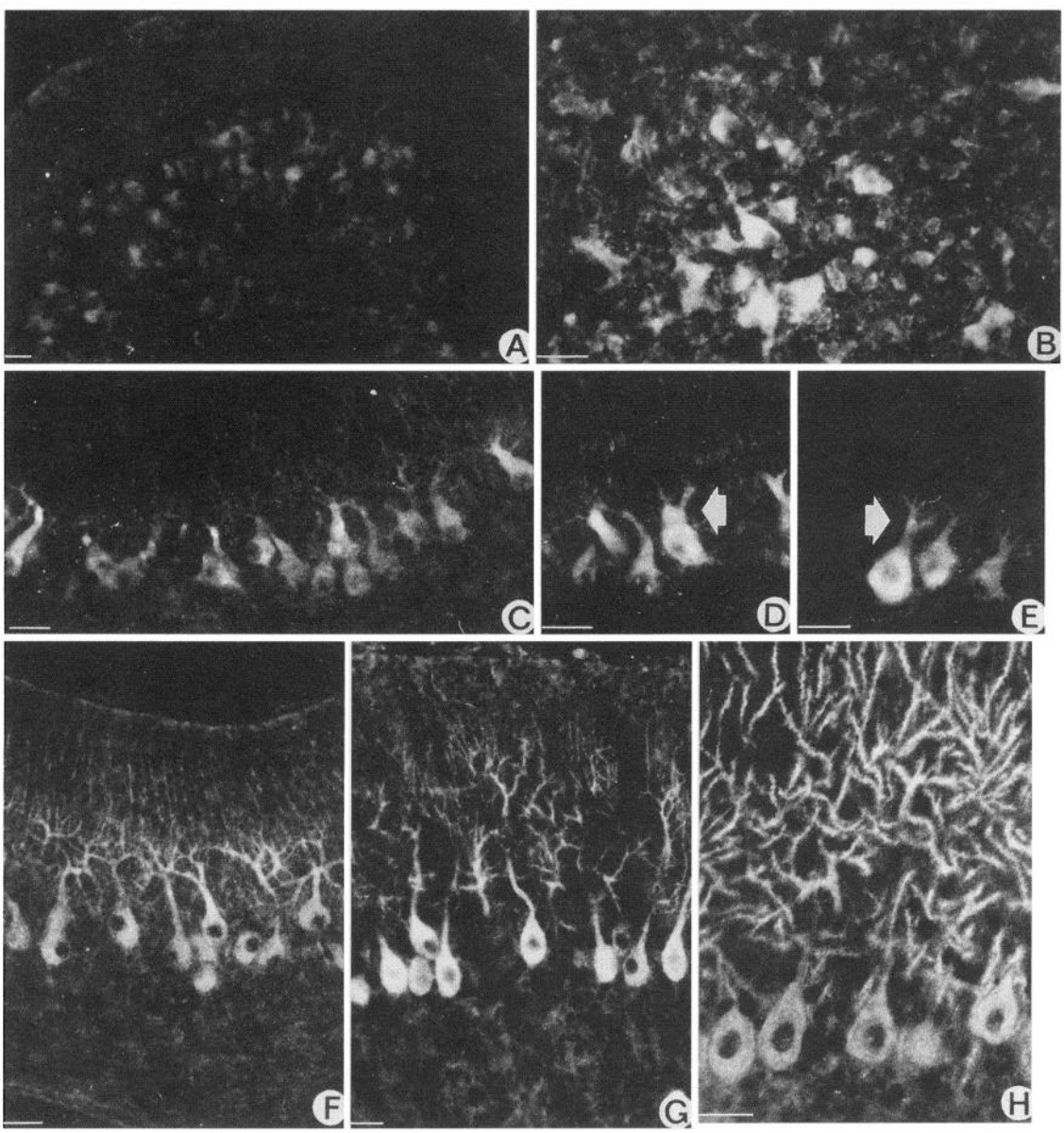

Fig. 2. Inositol 1,4,5-trisphosphate receptor (IP_3R) immunofluorescence of chicken Purkinje neurons. *A*: *E12*; *B*: *E11*; *C–E*: *E14*, Purkinje cell layer made up by immunolabeled pearlike cells; *F*: *E15*; *G*: *E18*; *H*: *P1*. Bar = 20 μm.

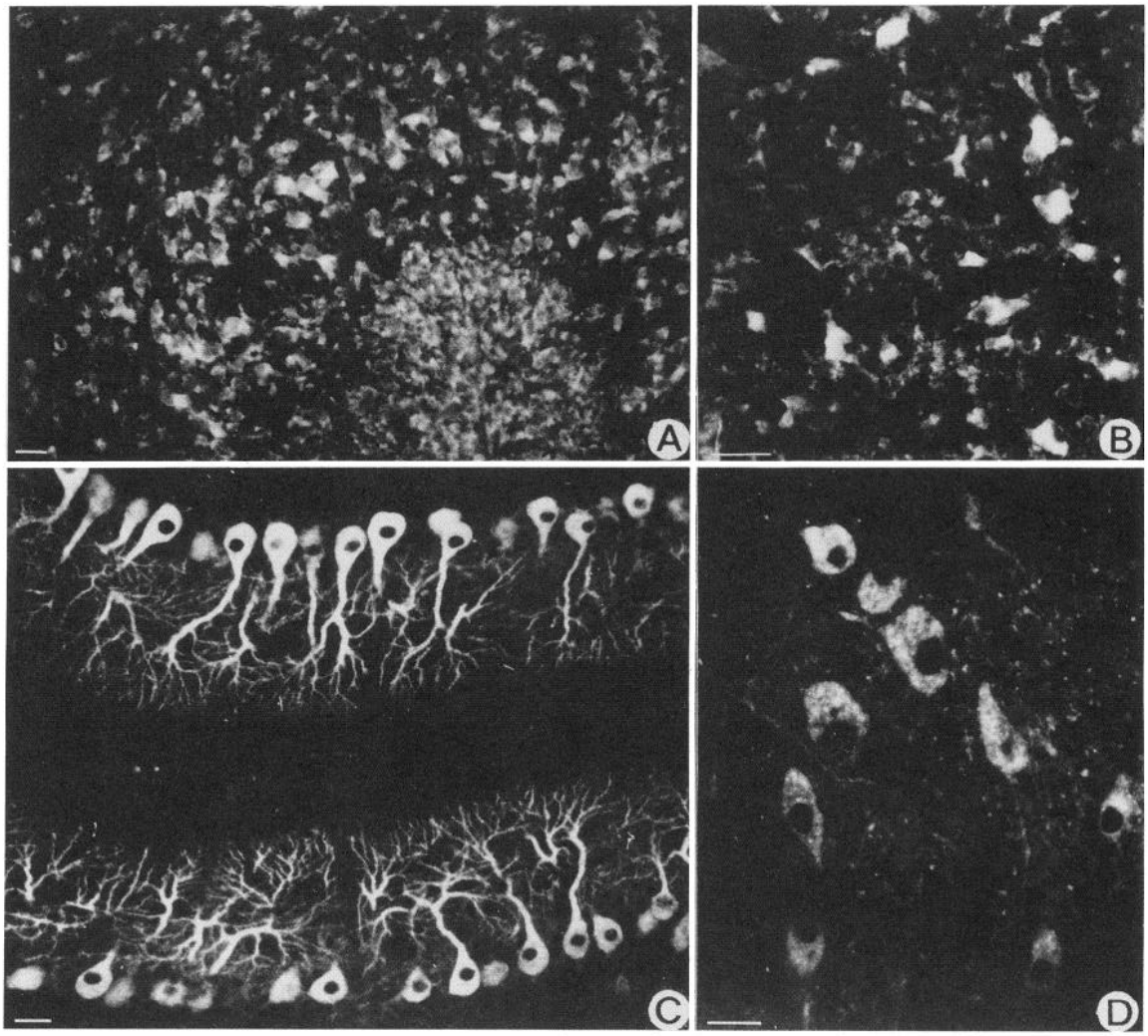

Fig. 3. Ca^{2+}-ATPase immunofluorescence of chicken cerebellum. *A* and *B*: *E11*; *C* and *D*: *E18*. *B* and *D* represent deep nuclei area; perikarya of nuclei are clearly labeled (cf. Ref. 28). Bar = 20 μm.

D and *E*). At *E21*, CS labeling is homogeneously observed at individual ER cisternae (Fig. 4*A*), whereas at *P2* and in the adult stage (Fig. 4, *B* and *C*, respectively) marked concentration of CS is found in elongated (arrowheads) or spherical (arrows) moderately electron-dense calciosomes. At *P2*, structures containing high levels of CS are first observed in the dendrites (Fig. 4*D*, arrowheads). Such structures appear elongated, different therefore from spherical electron dense vacuoles, as in the case of the adult stage (Fig. 4*E*, arrows).

IP_3R immugold labeling of the ER is evident already at *E18* (not shown) and persists at *E21*, *P2* (Fig. 4, *F* and *G*), and the adult stage (not shown; see Refs. 28, 35). The ER distribution of labeling is not homogeneous, with concentration in the well-known cisternal stacks that appear identical at all the stages investigated in both the soma (Fig. 4, *F* and *G*; see Refs. 28, 35) and dendrites (not shown).

Clues to the functional relevance of the morphological findings reported in Figs. 1–4 were sought in electrophysiological and microfluorimetric experiments carried out on single chicken Purkinje cells (Figs. 5–7).

Ionotropic receptors in single chicken Purkinje cells. Figure 5 shows three representative experiments carried out on dissociated single Purkinje cells at *E16–E17* in the presence of the preferred agonist for each subtype of the glutamate ionotropic receptor category. Figure 5, *A–C*, shows the membrane current recorded from a cell, maintained under voltage- and concentration-clamp conditions, to 100 μM *N*-methyl-D-aspartate (NMDA), 120 μM kainate (KA), or 50 μM quisqualate (QA), respectively. In Fig. 5*A*, the amount of desensitization was typically small and very slow. In Fig. 5*B*, as expected, no desensitization was observed. In Fig. 5*C*, the typical rapid desensitization was observed.

Taken together these results indicate that both NMDA and non-NMDA subtypes of excitatory amino acid ionotropic receptors are functional in Purkinje cells from *E16* to posthatching.

Metabotropic receptors and IP_3-sensitive Ca^{2+} stores in single chicken Purkinje cells. Redistribution of Ca^{2+} via IP_3R is due to activation of relevant plasma membrane receptors, such as the QA-type metabotropic glutamate receptor (12, 23), followed by the breakdown

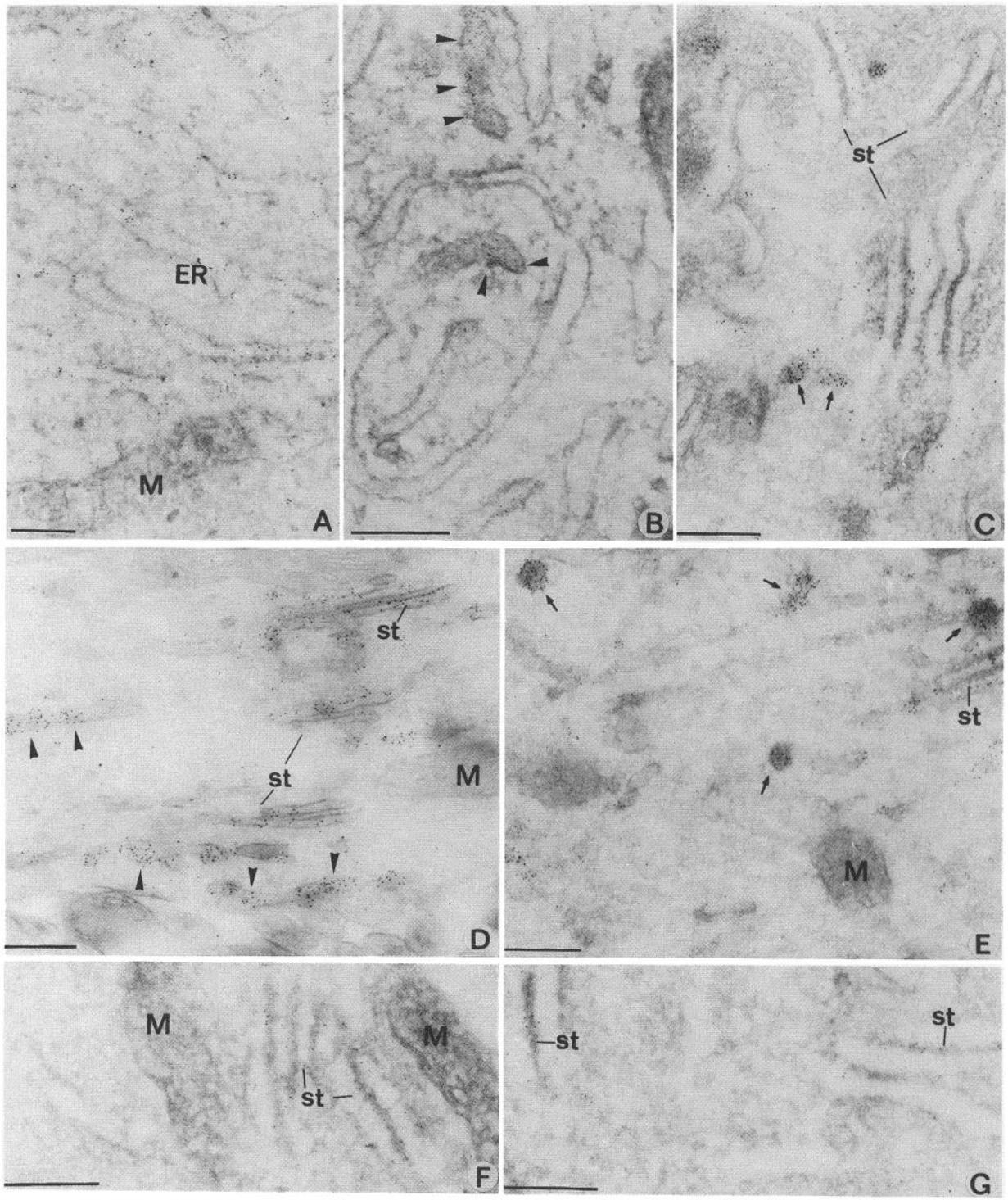

Fig. 4. Calsequestrin (CS) and IP_3R immunolabeling of Purkinje neurons (soma in *A–C*, *F*, and *G*; dendrite in *D* and *E*). *A–E*: CS immunolabeling; *F* and *G*: IP_3R immunolabeling. *A* and *F*: *E21*; *B*, *D*, and *G*: *P2*; *C* and *E*, adult stage. Arrowheads and arrows indicate CS-positive elongated or spherical membrane-bound structures exhibiting a moderately dense content. ER, endoplasmic reticulum; M, mitochondrion; st, stacks. Bar = 0.25 μm.

of phosphatidylinositol 4,5-bisphosphate into IP_3, a soluble intracellular second messenger, and diacylglycerol. ACPD, a selective metabotropic agonist with no effects on ionotropic receptors (13, 19), was used to ascertain whether metabotropic receptors were operative and IP_3-sensitive Ca^{2+} stores functional in embryonic Purkinje cells.

Fura 2-AM, a fluorescent cell-trappable Ca^{2+} indicator (6), was loaded into dissociated, single Purkinje cells plated on a coverslip, and cytoplasmic Ca^{2+} transients were monitored by microfluorimetry. Figure 6 shows a representative experiment in which application of ACPD (500 μM in picospritzer pipette) elicited a typical biphasic cytoplasmic Ca^{2+} transient, i.e., a spike followed by a

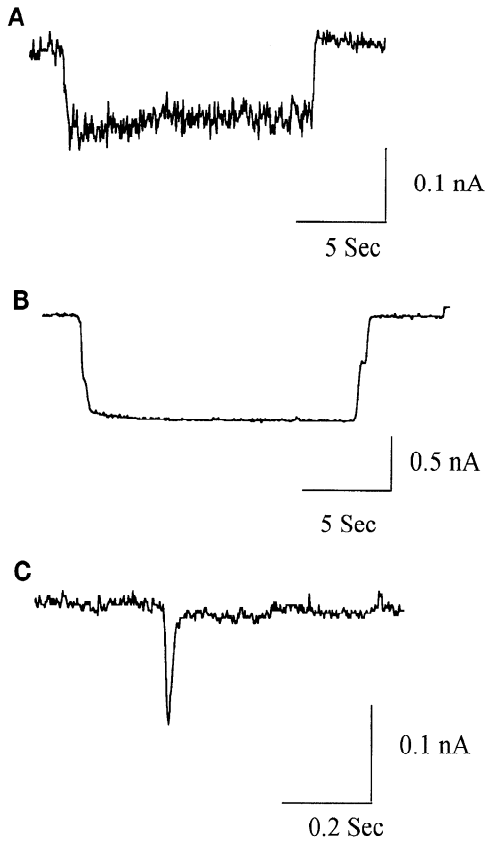

Fig. 5. Whole cell recordings of membrane currents in single Purkinje cells at *E16–E17* in response to ionotropic receptor agonists. Measurements of membrane currents were carried out as described in MATERIALS AND METHODS. *A*: *N*-methyl-D-aspartate (NMDA) and glycine (NMDA coagonist) concentrations were 100 and 2 μM, respectively; Purkinje cell was at *E17* and holding potential at −65 mV; 46 cells were tested, and 80% of them responded to NMDA. *B*: experiments were carried out in presence of 120 μM kainate (KA) and normal extracellular magnesium to block NMDA-gated channel; Purkinje cell was at *E17*; 24 cells were tested, and 96% of them responded to KA. *C*: quisqualate concentration was 50 μM, Purkinje cell was at *E16*. Note faster time scale for this trace; 6 cells were tested, and all of them responded.

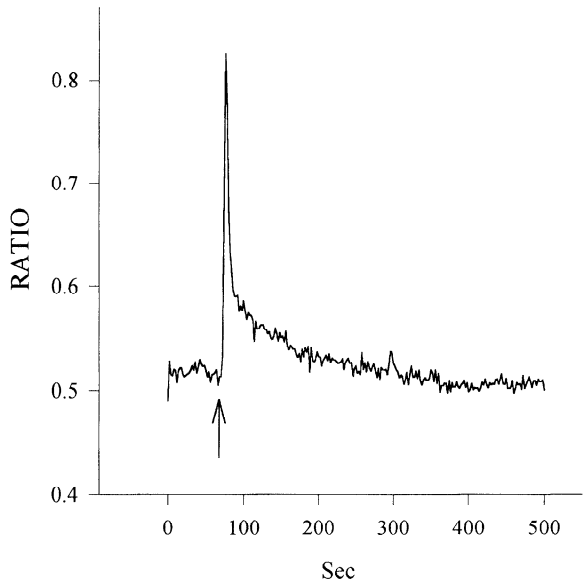

Fig. 6. Cytoplasmic Ca^{2+} transient elicited by *trans*-(1*S*,3*R*)-1-aminocyclopentane-1,3-dicarboxylic acid (ACPD) in a single Purkinje cell at *E19*. Experiments were carried out on 7 different cells as described in MATERIALS AND METHODS. ACPD (500 μM in pipette) was pressure ejected onto cell (arrow) for 10 s. Time course of Ca^{2+} transient was biphasic spike due to Ca^{2+} release from IP_3-sensitive Ca^{2+} stores and long-lasting tail due to Ca^{2+} influx from extracellular medium.

long-lasting tail. Clear evidence was thus gathered as to the coupling between metabotropic receptors and IP_3 receptors and the occurrence of IP_3-sensitive Ca^{2+} stores in embryonic Purkinje cells. It is noteworthy that previous attempts (3) to show IP_3-sensitive Ca^{2+} stores in cultured Purkinje cells from embryonic rat failed.

Caffeine-sensitive Ca^{2+} stores in single chicken Purkinje cells. Intracellular Ca^{2+} channels belong to two distinct categories, one sensitive to IP_3 and the other sensitive to caffeine, Ca^{2+}, and ryanodine (20). Evidence for the presence of the latter category of Ca^{2+} channels was obtained in single embryonic Purkinje cells as shown in Fig. 7.

A single fura 2-AM-loaded Purkinje cell was challenged with caffeine (10 mM in pipette) using a protocol of multiple sequential applications of the agonist (see legend to Fig. 7). Each application gave rise to a Ca^{2+} transient of decreasing amplitude, probably due to progressive Ca^{2+} store depletion (see Refs. 3, 11, 29). Alternative explanations, desensitization or adaptation of the caffeine-sensitive Ca^{2+} channel, are plausible but were not tested experimentally.

DISCUSSION

In the present study, three independent methodological approaches were implemented to investigate the

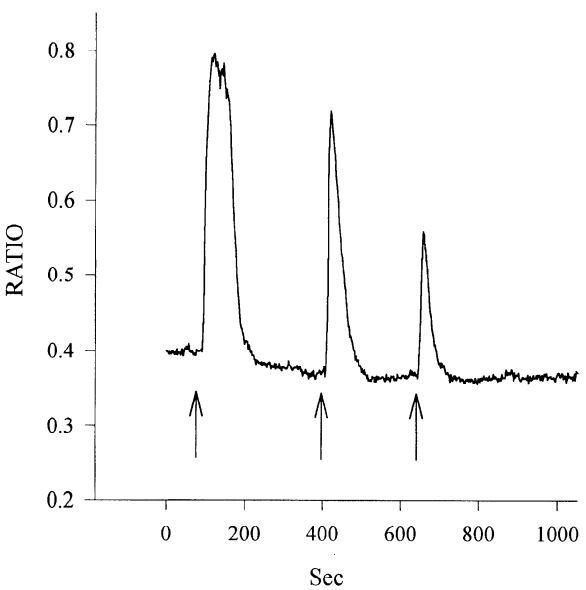

Fig. 7. Cytoplasmic Ca^{2+} transients elicited by caffeine in a single Purkinje cell at *E19*. Experiments were carried out on 12 different cells as described in MATERIALS AND METHODS. Caffeine (10 mM in pipette) was pressure injected onto cell. Each caffeine application (arrows) was of 60 s and oulasted Ca^{2+} release responses (upward deflections). Each Ca^{2+} transient had a similar time course although decreased in amplitude.

molecular composition and function of intracellular Ca^{2+} stores in chick Purkinje cells from *E11* onward.

We have observed by immunocytochemistry (Figs. 1–3) that *1*) CS, IP_3R, and Ca^{2+}-ATPase, the main constituents of intracellular rapidly exchanging Ca^{2+} stores, are first detected in Purkinje neurons during their migration across the cerebellum cortex; and *2*) a temporal correlation exists between well-known stages of cerebellum histogenesis and Purkinje cell morphological changes on the one hand and coexpression of CS, IP_3R, and Ca^{2+}-ATPase on the other.

Thus maturation of chick Purkinje neurons is attained around hatching, with respect also to Ca^{2+} stores. Cytogenesis and histogenesis, phenomena dictated by the character of the offspring, are accomplished in the chick much earlier than in mammalian cerebella (see Refs. 17, 34, 38).

Reprogramming of gene expression of cerebellum Purkinje neurons is required to bring about changes in cell position and morphology, including transformation of bipolar cells into stellate cells and dendritic branching. Analysis of transplants, chimaeras, mutants, and transgenic animals has clearly indicated that Purkinje cells follow a stereotypical developmental map that is largely dictated by cell-intrinsic mechanisms (25–27, 39).

As to the biogenesis of membrane subcompartments specialized for intracellular Ca^{2+} homeostasis, expression of CS, Ca^{2+}-ATPase and IP_3R in migrating Purkinje cells (*E11–E12*) might indicate that the phenomenon is guided by cell-intrinsic mechanisms. Immunogold electron-microscopic studies (Fig. 4) indicate that around hatching both CS and IP_3R are attaining their definitive subcellular organization. Moreover, localization of Ca^{2+} store markers not only in the soma but also in the growing dendrites suggests that redistribution of Ca^{2+} from intracellular Ca^{2+} stores, along with transient Ca^{2+} influx across the plasma membrane, is involved not only in the regulation of cell migration but also in that of dendritic branching.

A temporal coincidence in fact exists among the emergence of electrical activity in Purkinje neurons, the beginning of dendritic branching, and the changes in the characteristics of intracellular Ca^{2+} regulation (24). It has been also suggested that "dendritic elongation is the default growth pattern in Purkinje neurons and that this is overriden by activity-dependent alterations in calcium homeostasis," i.e., that "calcium transients could be a local signal shaping growth pattern" (24). Moreover, survival-promoting and survival-limiting effects on Purkinje neurons are accomplished in vitro through stimulation of metabotropic and ionotropic receptors, respectively (15), which in turn affect cytoplasmic Ca^{2+} concentration via distinct mechanisms (see below).

It can thus be proposed that one of the molecular events underlying morphological and functional maturation of Purkinje neurons is the turning on of genes coding for components of the rapidly exchanging Ca^{2+} stores. The hypothesis appears plausible based on electrophysiological and fluorimetric experiments carried out on acutely dissociated, single Purkinje neurons (Figs. 5–7).

First, it is known that afferent projections to cerebellum, i.e., functional circuitry, are established concomitantly with dendritic outgrowth (10) and that excitation of Purkinje neurons is mediated by excitatory amino acids via both ionic mechanisms and second messengers effects (23). All relevant ionotropic and metabotropic receptors and related pathways appear to be functional in chick Purkinje neurons well before hatching as shown in Figs. 5 and 6.

Second, chick embryo Purkinje neurons display cytoplasmic Ca^{2+} transients due to release from intracellular Ca^{2+} stores after agonist (ACPD) activation of QA-type metabotropic glutamate receptors as shown in Fig. 6. Because ACPD has no effect on ionotropic receptors (13), it is reasonable to conclude that IP_3 is responsible for inducing Ca^{2+} transients.

Third, yet another component of intracellular Ca^{2+} stores, the ryanodine receptor and/or Ca^{2+} release channel (5, 36), is present and functional in embryonic chick Purkinje neurons as indicated by caffeine-induced cytoplasmic Ca^{2+} transients (Fig. 7).

Thus Ca^{2+} stores by controlling, at least in part, cytoplasmic Ca^{2+} concentration may be involved in specific histogenetic and morphogenetic events, e.g., cell migration and dendrite branching. The specific roles of intracellular Ca^{2+} stores in Purkinje neurons of embryonic chicks, however, remain to be fully ascertained in future experiments and may very well be multiple as implied here.

Finally, we have shown the occurrence of functional intracellular Ca^{2+} stores in a handy preparation of embryonic Purkinje cells with clear advantages over analogous preparations, derived from the rat (3), which were reported to display IP_3 and ryanodine receptors, judged by immunofluorescence, caffeine-sensitive Ca^{2+} stores, judged by microfluorimetry, and not to respond to ACPD, i.e., lack of coupling between metabotropic receptors and IP_3 receptors. The chick Purkinje cell preparation is therefore more suitable to address many relevant questions in the field of Ca^{2+} homeostasis, namely, the interplay within the same cell of IP_3-sensitive and caffeine-sensitive Ca^{2+} stores, and their physical relationships, i.e., separate or continuous compartments (20).

We thank Dr. D. M. Fambrough for the generous gift of monoclonal antibodies specific for the Ca^{2+}-ATPase and Drs. A. Margreth and J. Meldolesi for critical reading of the manuscript.

This work was supported by National Institute of Neurological Disorders and Stroke Grant NS-29640-02.

Present address of K. D. Cliffer: Regeneron Pharmaceuticals, 777 Old Saw Mill River Rd., Tarrytown, NY 10591.

Address for reprint requests: P. Volpe, Dipt. di Scienze Biomediche Sperimentali, Università di Padova, Via Trieste 75, 35121 Padua, Italy.

Received 5 December 1994; accepted in final form 19 April 1995.

REFERENCES

1. **Armengol, J.-A., and C. Sotelo.** Early dendritic development of Purkinje cells in the rat cerebellum. A light and electron microscopic study using axonal tracing in "in vitro" slices. *Dev. Brain Res.* 64: 95–114, 1991.

2. **Baffoni, G. M.** Osservazioni sulla morfogenesi e istogenesi del cevelletto di uccelli e sul ciclo vitale dei neuroni cerebellari. *Riv. Neurobiol. Perugia* 9: 453–580, 1963.
3. **Brorson, J. R., D. Bleakman, S. J. Gibbons, and R. J. Miller.** The properties of intracellular calcium stores in cultured rat cerebellar neurons. *J. Neurosci.* 11: 4024–4043, 1991.
4. **Campbell, A. M., F. Wuitack, and D. M. Fambrough.** Differential distribution of the alternative forms of the sarcoplasmic/endoplasmic reticulum Ca^{2+}-ATPase, SERCA2b and SERCA2a, in the avian brain. *Brain Res.* 605: 67–76, 1993.
5. **Ellisman, M. H., T. J. Deerinck, Y. Ouyang, C. F. Beck, S. J. Tanksley, P. D. Walton, J. A. Airey, and J. L. Sutko.** Identification and localization of ryanodine binding proteins in the avian central nervous system. *Neuron* 5: 135–146, 1990.
6. **Grinkievicz, G., M. Poenie, and R. Y. Tsien.** A new generation of Ca^{2+} indicators with greatly improved fluorescent properties. *J. Biol. Chem.* 260: 3440–3450, 1985.
7. **Hallonet, M. E. R., M.-A. Teillet, and N. M. Le Douarin.** A new approach to the development of the cerebellum provided by the quail-chick marker system. *Development* 108: 19–31, 1990.
8. **Hamill, O. P., A. Marty, E. Neher, B. Sakmann, and F. J. Sigworth.** Improved patch-clamp techniques for high resolution current recording from cells and cell-free membrane particles. *Pfluegers Arch.* 391: 85–100, 1981.
9. **Kaprielian, Z., A. M. Campbell, and D. M. Fambrough.** Identification of a Ca^{2+}-ATPase in cerebellar Purkinje cells. *Mol. Brain Res.* 6: 55–60, 1989.
10. **Kawamura, K., and T. Hashikawa.** Olivo-cerebellar projections in the cat studied by means of antrograde axonal transport of labelled aminoacids tracers. *Neuroscience* 4: 1615–1635, 1979.
11. **Libscombe, D., D. W. Madison, M. Poenie, H. Reuter, R. W. Tsien, and R. Y. Tsien.** Imaging of cytosolic Ca^{2+} transients arising from Ca^{2+} stores and Ca^{2+} channels in sympathetic neurons. *Neuron* 1: 355–365, 1988.
12. **Llano, I., J. Dressen, M. Kano, and A. Konnerth.** Intradendritic release of calcium induced by glutamate in cerebellar Purkinje cells. *Neuron* 7: 577–583, 1991.
13. **Manzoni, O., L. Fagni, J.-P. Pin, F. Rassendren, F. Poulat, F. Sladeczek, and J. Bockaert.** (*Trans*)-1-amino-cyclopentyl-1,3-dicarboxylate stimulates quisqualate phosphoinositide-coupled reptors but not ionotropic glutamate receptors in striatal neurons and *Xenopus* oocytes. *Mol. Pharmacol.* 38: 1–6, 1990.
14. **Michelangeli, F., F. Di Virgilio, A. Villa, P. Podini, J. Meldolesi and P. Pozzan.** Identification, kinetic properties and intracellular localization of the (Ca^{2+}-Mg^{2+}) ATPase from the intracellular stores of chicken cerebellum. *Biochem. J.* 275: 255–261, 1991.
15. **Mount, H. T. J., C. F. Dreyfus, and I. B. Black.** Purkinje cell survival is differentially regulated by metabotropic and ionotropic excitatory amino acid receptors. *J. Neurosci.* 13: 3173–3179, 1993.
16. **Mugnaini, E.** Ultrastructural studies on the cerebellar histogenesis. II. Maturation of nerve cell populations and establishments of synaptic connections in the cerebellar cortex of the chick. In: *Neurobiology of Cerebellar Evolution and Development*, edited by R. Llinas. Chicago, IL: AMA, 1969, p. 749–782.
17. **Nakanishi, S., N. Maeda, and K. Mikoshiba.** Immunohistochemical localization of an inositol 1,4,5-trisphosphate receptor, p400, in neural tissues: studies in developing and adult mouse brain. *J. Neurosci.* 11: 2075–2086, 1991.
18. **Nori, A., A. Villa, P. Podini, D. R. Witcher, and P. Volpe.** Intracellular Ca^{2+} stores of rat cerebellum: heterogeneity within and distinction from endoplasmic reticulum. *Biochem. J.* 291: 199–204, 1993.
19. **Palmer, D., D. T. Monagham, and C. W. Cotman.** *Trans*-ACPD, a selective agonist of the phosphoinositide-coupled excitatory amino acid receptor. *Eur. J. Pharmacol.* 166: 585–587, 1989.
20. **Pozzan, T., R. Rizzuto, P. Volpe, and J. Meldolesi.** Molecular and cellular physiology of intracellular Ca^{2+} stores. *Physiol. Rev.* 74: 595–636, 1994.
21. **Ramon y Cajal, S.** Sobre ciertos elementos bipolares del cerbelo joven y algunos detalles mas acerca del crecimiento y evolucion de las fibras cerebelosas. *Gac. Sanit. Barcelona* 10: 1–20, 1890.
22. **Ramon y Cajal, S.** *Histologie du Systeme Nerveux de l'Homme et des Vertebrates.* Paris: Maloine, 1911, vol. 2.
23. **Ross, C. A., D. Bredt, and S. H. Snyder.** Messengers molecules in cerebellum. *Trends Neurosci.* 13: 216–222, 1990.
24. **Schilling, K., M. H. Dickinson, J. A. Connor, and J. I. Morgan.** Electrical activity in cerebellar cultures determines Purkinje cell dendritic growth patterns. *Neuron* 7: 891–902, 1991.
25. **Smeyne, R. J., and D. Goldowitz.** Postnatal development of the wild-type and weaver cerebellum after embryonic administration of propylthiouracil (PTU). *Dev. Brain Res.* 52: 211–222, 1990.
26. **Smeyne, R. J., J. Oberdick, K. Schilling, A. S. Berrebi, E. Mugnaini, and J. I. Morgan.** Dynamic organization of developing Purkinje cells revealed by transgene expression. *Science Wash. DC* 254: 719–721, 1991.
27. **Sotelo, C., and R. M. Alvarado-Mallart.** Reconstruction of the defective cerebellum circuitry in adult Purkinje cell degeneration mutant mice by Purkinje cell replacement through transplants of solid embryonic implants. *Neuroscience* 20: 1–22, 1987.
28. **Takei, K., H. Stukenbrok, A. Metcalf, G. A. Mignery, T. C. Sudhof, P. Volpe, and P. De Camilli.** Ca^{2+} stores in Purkinje neurons: endoplasmic reticulum subcompartments demonstrated by the heterogeneous distribution of the $InsP_3$ receptor, Ca^{2+}-ATPase and calsequestrin. *J. Neurosci.* 12: 489–505, 1992.
29. **Thayer, S. A., M. Sturek, and R. J. Miller.** Measurements of neuronal Ca^{2+} transients using simultaneous microfluorimetry and electrophysiology. *Pfluegers Arch.* 412: 246–223, 1988.
30. **Villa, A., P. Podini, D. O. Clegg, T. Pozzan, and J. Meldolesi.** Intracellular Ca^{2+} stores in chicken Purkinje neurons: differential distribution of the low-affinity high-capacity Ca^{2+} binding protein, calsequestrin, of Ca^{2+}-ATPase and of the ER lumenal protein Bip. *J. Cell Biol.* 113: 779–791, 1991.
31. **Volpe, P., B. H. Alderson-Lang, L. Madeddu, E. Damiani, J. H. Collins, and A. Margreth.** Calsequestrin, a component of the inositol 1,4,5-trisphosphate-sensitive Ca^{2+} store of chicken cerebellum. *Neuron* 5: 713–721, 1990.
32. **Volpe, P., S. Furlan, and E. Damiani.** Purification and characterization of calsequestrin from chicken cerebellum. *Biochem. Biophys. Res. Commun.* 181: 28–35, 1991.
33. **Volpe, P., L. Gorza, M. Brini, R. Sacchetto, S. Ausoni, and D. O. Clegg.** Expression of the calsequestrin gene in chicken cerebellum Purkinje neurons. *Biochem. J.* 294: 487–490, 1993.
34. **Volpe, P., R. Sacchetto, and B. H. Alderson-Lang.** Postnatal expression of the inositol 1,4,5-trisphosphate receptor in canine cerebellum. *Int. J. Biochem.* 24: 1525–1532, 1992.
35. **Volpe, P., A. Villa, E. Damiani, A. H. Sharp, P. Podini, S. H. Snyder, and J. Meldolesi.** Heterogeneity of microsomal Ca^{2+} stores in chicken Purkinje neurons. *EMBO J.* 10: 3183–3188, 1991.
36. **Walton, P. D., J. A. Airey, J. L. Sutko, C. F. Beck, G. A. Mignery, T. C. Sudhof, T. J. Deerinck, and M. H. Ellisman.** Ryanodine and inositol trisphosphate receptors coexist in avian cerebellar Purkinje neurons. *J. Cell Biol.* 113: 1145–1153, 1991.
37. **Wassef, W., J. P. Zanetta, A. Brehier, and C. Sotelo.** Transient biochemical compartmentalization of Purkinje cells during early cerebellar development. *Dev. Biol.* 111: 129- 137, 1985.
38. **Worley, P. F., J. M. Baraban, and S. H. Snyder.** Inositol 1,4,5-trisphosphate-recepotor in brain. Autoradiographic localization in brain. *J. Neurosci.* 9: 339–346, 1989.
39. **Wuenschell, C. W., and A. J. Tobin.** The abnormal cerebellar organization of *Weaver* and *reeler* mice does not affect the cellular distribution of three neuronal mRNAs. *Neuron* 1: 805–815, 1988.